

Arvind Singh Negi,

Evaluation of the Mycogenic Biosynthesis of Silver Nanofungicides' Efficacy against Blight Disease Infestations of *Phytophthora Infestans* and *Alternaria Soloni* in Potato *Solanum Tuberosum*

# Evaluation of the Mycogenic Biosynthesis of Silver Nanofungicides' Efficacy against Blight Disease Infestations of *Phytophthora Infestans* and *Alternaria Soloni* in Potato *Solanum Tuberosum*

Arvind Singh Negi

Asst. Professor, School of Agriculture, Graphic Era Hill University, Dehradun Uttarakhand India

## Abstract

This research evaluates the efficacy of chemical fungicides against nanofungicides in protecting Potato crops from Early and Late Blight. With the help of the IARI-ITCC, diseased solanaceous vegetables were gathered for the purpose of isolating early and late blight pathogens (*Alternaria solani* and *Phytophthora infestans*, respectively). *Aspergillus niger* and *A. flavus* biomass at 100 mg and 1 gm biomass per ml concentrations, respectively, were used as a catalyst for the production of silver and zinc oxide nanoparticles in the presence of silver nitrate and zinc nitrate precursor salts. The sizes, shapes, and concentrations of synthesised nanoparticles were determined using UV-Vis spectroscopy, FESEM, EDX, FTIR, DLS, AFM, and ICPMS. Silver and zinc oxide nanoparticles were tested in vitro against *A. solani* and *P. infestans* to determine their minimum inhibitory concentration. Using UV-Vis spectroscopy and FTIR, we analysed the process by which microbes and metals interact in reaction conditions.

**Keywords:** *Mycogenic Biosynthesis, Silver Nanofungicides', Blight Disease, Phytophthora Infestans, Alternaria Soloni, Potato Solanum Tuberosum.*

**Tob Regul Sci.™ 2021;7(4): 533-545**

**DOI: <https://doi.org/10.52783/trs.v7i4.1307>**

## 1. Introduction

One of the most widely consumed and commercially valuable members of the solanaceae family is the potato (*Solanum tuberosum* L.). tiny tubers or cuttings from larger tubers that have developed tiny eyes are employed for this purpose. In 2004, over 80% of the world's potato crop was grown in European and Asian nations, from where output surged dramatically to a total of 374 metric tonnes. The Chinese are the world's largest producer of potatoes, followed by the Indians and the Russians. Vegetables are in high demand all year long because of their key role in the human diet. Vitamins, minerals, antioxidants, bioflavonoids, flavour compounds, and dietary fibre are all rapidly destroyed by abiotic and biotic stresses, and perishables are particularly vulnerable. The versatile potato serves as both a delicious food and a useful ingredient in a wide variety of manufactured goods. The fresh tubers of a potato consist of around 20% dry matter

Arvind Singh Negi,

Evaluation of the Mycogenic Biosynthesis of Silver Nanofungicides' Efficacy against Blight Disease Infestations of *Phytophthora Infestans* and *Alternaria Soloni* in Potato *Solanum Tuberosum*

and 80% water. Starch accounts for almost 75% of the dry matter, with protein, fibre, and even some fatty acids rounding out the composition.[1-2]

### 1.1 Potato Disease

There are around 160 illnesses and disorders that might affect potato output. Fungi, bacteria, and viruses are each responsible for 50, 10 and 40, respectively. Many different types of biotic and abiotic illnesses may affect crops of *Solanum tuberosum* L., and the primary types of abiotic stress in potato production include zinc deficiency, salt, acidic pH, and high temperature. Reduced starch content and a lack of nitrogen both delay tuber development and increase the likelihood of peeling and bruising during harvest. Some diseases may be more easily transmitted to a potato plant in conditions of low fertility and abiotic water stress.[3]

Viruses, nematodes, bacteria, and fungus are only some of the many plant diseases that have been described as major pests of the potato crop. Late blight, ring rot, early blight, and leaf roll are the most destructive and severe diseases of potato crop, capable of wiping out an entire harvest. Fungal infections play a crucial part in production losses and may affect a plant in three different ways: via the leaves, the soil, and the tubers.[4]

### 1.2 Early blight disease of Potato

In order to protect their crop against infections like *Alternaria solani* and *Phytophthora infestans*, potato farmers must deal with a number of pests and diseases. In the potato industry, early blight is a major concern since it may destroy a crop by itself or in tandem with other damaging diseases like late blight if not managed well. Both *Alternaria solani* (Jones & Grouet) and *A. alternata* (Fr.) Keissler are pathogens that may cause early blight of potatoes, although the former is generally considered to be more responsible. They pose a significant risk to potato cultivation because their spores are ubiquitous in the environment and may easily spread when environmental circumstances are favourable for infection.[5-6]

The phrase "early blight disease of potato" because it strikes more on early maturing cultivars than on medium or late maturing ones. Potato foliage is a common target for the viruses, leading to the disease's other name: senescence. The spores of this fungus may live in the soil for years, and infected dried leaves and potato detritus (leaves and tubers) might serve as a key infection source. Conidia are spore-like reproductive structures of fungi that are spread by water, wind, and insects and may enter hosts either directly or indirectly via the stomata. In India, early blight causes 40% yield losses, and the circumstances that support its development—regularly changing weather, i.e. showers or ample moisture followed by dry and warm weather—are not ideal for the potato crop.[7]

Arvind Singh Negi,

Evaluation of the Mycogenic Biosynthesis of Silver Nanofungicides' Efficacy against Blight Disease Infestations of *Phytophthora Infestans* and *Alternaria Solani* in Potato *Solanum Tuberosum*

## 2. Literature review

**Paquot, M. and Rouxhet, P.G., (2021)** Traditional landrace (indigenously cultivated) populations growing in lowland Chile and the high Andes are known as *Solanum tuberosum*. The wild potato species *Solanum Petota* and related landrace potatoes are employed in crop improvement and categorization efforts. Species belonging to section *petota* may be found all the way from the southwestern United States to the southernmost parts of South America. The potato is a very adaptable crop that can be produced in a wide range of climates and is thus often exported to nations such as Chile, China, Brazil, etc. The potato (*Solanum tuberosum* L.) is the third most significant food crop because of its widespread cultivation and use as a staple meal. Perishable foods are a vital element of a healthy diet, but they are vulnerable to abiotic and biotic stresses such as spoilage, rotting, and insect infestation.[8]

**Kumar, R. and Sastry, M., (2020)** Pests and diseases may easily damage a potato crop, and the plant is also susceptible to damage from frost, hail, drought, and even nutritional deficits and toxicity. Although there are many pests and illnesses that may damage potatoes, late blight is the most pervasive and has caused the greatest damage to potatoes ever since the Irish potato famine. When it comes to fungal diseases, phytopathologists are most concerned about early and late blight since it reduces potato output worldwide and is responsible for an estimated €12 billion in lost tuber yields. Crops that are poorly nourished or have no disease prevention measures in place are more likely to experience early and late blight. It is estimated that late blight may reduce output by anywhere from 10 to 85% depending on the weather, with a nationwide average loss of 15%.[9]

**Supriyanto, G. and Zaidan, A.H., (2019)** *M. A. Solani* Eukaryota, Kingdom Fungi, Phylum Deuteromycota, Class Hyphomycetes, Order Hyphales, Series Porosporae; taxonomy, morphology, and culture. The morphology of *A. solani* colonies is often abundant, greyish brown to black, and has the appearance and feel of cotton, felt, or velvet. Nuclear division in hyphal cells results in multiple multinucleated cells, and the number of nuclei varies throughout the organs of *A. solani*. A shade of olive brown Conidiophores are up to 110 μm in length and 6–10 μm in diameter; they are thick-walled, straight to flexuous, septate, emerge individually or in small groups, and Conidiogenesis is tragic. Conidia range in size from 75 to 350 μm in length and 20 to 30 μm in diameter and may be anywhere from a pale yellow to an olivaceous brown colour. They are normally found alone or in short chains.[10]

**Oliveira, G. and Góes-Neto, A., (2018)** Several cycles of infection and disease severity by the *A. solani* pathogen are conceivable in potato and tomato crops during the growing season. Overwintering inoculum is the primary source of infections in freshly planted potatoes. Mycelium or conidia of the pathogen overwinter in plant detritus, soil, and diseased tubers, or on other host plants of the same family. Overwintering inoculum sources, such as chlamydospores,

Arvind Singh Negi,

Evaluation of the Mycogenic Biosynthesis of Silver Nanofungicides' Efficacy against Blight Disease Infestations of *Phytophthora Infestans* and *Alternaria Solani* in Potato *Solanum Tuberosum*

have also been observed for early blight, enabling the pathogen to withstand freezing soil temperatures. Debris in uncultivated soil may harbour the inoculum for up to eight months, and the hyphae's dark pigmentation makes them resistant to lysis. Spores of the fungus are more likely to endure in contaminated detritus and seed, where their chances of survival are mostly determined by meteorological, edaphic, and biotic variables.[11]

**Kim, B.I. and Adair, J.H., (2017)** Infections with early blight (*Alternaria solani* Sorauer), among other diseases and pests, may lower production by as much as 20%. The foliar sprays of Boscalid + Pyraclostrobin were not only successful in preventing the spread of the disease, but they also had a beneficial effect on crop production, quality, and survival of processing cultivars. There was a significant upregulation of stress oxidative enzymes and phytoalexins defence mechanisms in Boscalid + Pyraclostrobin-treated tubers, including two crucial peroxidase and polyphenol oxidase enzymes. Increased deposition of cell wall reinforcing components such as phenols and lignin was also seen in Boscalid + Pyraclostrobin treated tubers. Management of these types using chemical fungicides, such as Boscalid + Pyraclostrobin, helps preserve the foliage, boosts production and quality, and encourages the development of systemic acquired resistance, which enhances the tuber's capacity to be stored.[12]

### 3. Methodology

#### 3.1 Isolation and characterization of some plant pathogenic fungal species from the solanaceous vegetable of Western Uttar Pradesh.

##### 3.1.1 Collection of vegetable samples

For the purpose of isolating the fungi responsible for the blight disease, infected plant materials of potatoes showing black-brown spots were collected in sterile polythene bags from various agricultural fields of CPRI modipuram and the research field of the department of Genetics and Plant Breeding, Chaudhary Charan Singh University, Meerut between January 2020 and March 2020. Those diseased sections of vegetables that were collected were diced and washed in double-distilled water three to four times. The plant matter was also subjected to a 30-second soak in 70% ethanol and a 5-minute soak in a 1% sodium hypochlorite solution. Fungi were allowed to grow on the affected sections of the leaves for two or three days in a humidity room.

##### 3.1.2 Analysis of vegetable samples for mycobiota

Fungi were isolated from potatoes using potato dextrose agar (PDA) and Sabouraud Dextrose agar (SDA). About 200 grams of potatoes were peeled, sliced, and cooked for 30 minutes in 500 milliliters of purified water. After straining the broth through muslin, we added distilled water to bring the total volume to 1 liter. According to the 1000 ml of medium, agar and dextrose were added. The solution's pH was lowered to 6.7. The medium was then autoclaved at 121 degrees

Arvind Singh Negi,

Evaluation of the Mycogenic Biosynthesis of Silver Nanofungicides' Efficacy against Blight Disease Infestations of *Phytophthora Infestans* and *Alternaria Soloni* in Potato *Solanum Tuberosum*

Celsius for 30 minutes to kill any bacteria. In a similar vein, the components listed in table 3.2 were used to concoct the SDA medium. Before usage, the Petri dishes and other glassware were disinfected in a hot-air oven at 160 degrees Celsius for three hours. In addition, 40mg/l of ampicillin and streptomycin antibiotics were added to the medium before it was poured onto petri plates to inhibit the development of bacteria. Petri plates were incubated at 25 1.0 °C for 6-8 days after having sample inoculated into the medium.

### 3.1.3 Identification of fungi

A drop of lacto phenol cotton blue was placed on a glass slide, a piece of the fungal colony was removed from the sub-structured plates and transferred to the slide using a sterile inoculating needle, the colony was emulsified using the same needle, and the slide was carefully covered with a coverslip to prevent air bubbles. Microscopical examination of the colony was performed in accordance with the description given in *The Identification of Fungi: An Illustrated Introduction with Keys, Glossary, and Guide* by Frank M. Dugan, and included searching for various features of fungi such as hyphae, conidia, and sporangiophore (reproductive structure). The isolated fungus was identified using up-to-date identification keys and appropriate conditions, slide cultures, and inverted phase-contrast microscopy spore examinations. Fungi were confirmed and identified to the species level by sending samples to the Indian Type Culture Collection (IARI-ITCC) in New Delhi.

### 3.2 Study of microbe-metal interaction mechanism through UV-Vis spectroscopy and FTIR.

To learn about the kinetic behavior of nanoparticles and to interpret their interaction with fungal biomass, UV-Vis spectra were collected and analyzed at room temperature in a quartz cell with a 1 cm optical path. The samples were scanned between 200 and 800 nm. UV prov software was installed on the spectrophotometer for data recording and analysis. A blank reference was used to do the baseline correction on the spectrophotometer.

About 15 ml of liquid samples were dried on petri dishes with biomass in a hot air oven at 70°C for 48 hours in order to perform FTIR analysis. The interaction of fungal macromolecules with metal nanoparticles was studied using the Fourier transform infrared (FTIR) capability at the Sophisticated Analytical Instrument capability (SAIF), Indian Institute of Technology (IIT), Bombay. The spectra of absorption were collected from 4000 cm<sup>-1</sup> to 400 cm<sup>-1</sup>. To facilitate further analysis, solid samples were crushed with potassium bromide (about 5%) and pressed to produce a firm pellet. The wavelength of interference patterns is determined by passing the radiation from an infrared source through an interferometer with a beam splitter, a fixed mirror, and a moving mirror. The intensity of the incident radiation at a certain wave number was measured in order to construct an infrared spectrum.

Arvind Singh Negi,

Evaluation of the Mycogenic Biosynthesis of Silver Nanofungicides' Efficacy against Blight Disease Infestations of *Phytophthora infestans* and *Alternaria solani* in Potato *Solanum Tuberosum*

#### 4. Results

##### 4.1 Isolation and characterization of some plant pathogenic fungal species from the solanaceous vegetable of Western Uttar Pradesh.

###### 4.1.1 Isolation and characterization

Subcultures and pure cultures were created from the various fungal colonies growing on the medium. *Phytophthora infestans*, *Alternaria solani*, *Aspergillus versicolor*, and *Fusarium oxysporum* (table 4.1) are the four fungal species that were isolated and identified by microscopic examinations and subsequently validated by IARI- ITCC. In particular, the two fungi (*A. solani* and *P. infestans*) that are responsible for early and late blight of potato were of interest. Table 4.2 lists the observed and analyzed morphological features.

Table 4.1: Diseases induced by the isolated fungus species on solanaceae plants

Fungi	Disease	Symptoms	References
<i>P. infestans</i>	Late blight	Large areas of foliage and fruits develop hard, brown, round patches.	Andrivon, 1995; Haverkort et al, 2009; Nowicki et al, 2012;
<i>A. solani</i>	Early blight	At first, just a few tiny black spots will appear on older leaves that are low to the ground. Target-like concentric circles may be seen around the larger areas.	Chaerani and Voorrips, 2006; Horsfield et al, 2010; Kumar and Srivastava, 2013
<i>A. versicolor</i>	-	Fungal endophytes	Paul et al, 2012; Nakayama, 2017; Rana et al, 2019;

Table 4.2: Isolated fungi's defining morphological features

Fungal species	macro-morphological characteristics	micro-morphological characteristics
<i>P. infestans</i>	Mycelium that was white-brown in color, fluffy, and abundantly branching was grown on agar plates.	Lemon-shaped, semipapillate sporangia that contained zoospores were also detected, as well as aseptate mycelium.
<i>A. solani</i>	resulted in the development of a woolly, hairy coat that is various shades of grey, black, and brown.	Fungus conidiophores were developed singly or in clusters, straight or flexuous, brown to olivaceous, muriform, ellipsoidal, and tapering to a beak.
<i>A. versicolor</i>	Resulted in white colonies whose development included multiple radial grooves or folds	Septate and hyaline hyphae were spotted. The radiating conid heads were bisect. These fungi have hyaline, wallless conidiophores.
<i>F. oxysporum</i>	resulted in light yellow cottony mycelia.	Canoe-shaped spores were seen.

*P. infestans* produces its asexual spores in microscopic structures called sporangia. These sporangia measure between 20 and 40  $\mu$ m in length, are completely see-through, and have the shape of a lemon. When the relative humidity or water content of the environment is high, the cytoplasm of the sporangia splits and several free-swimming zoospores are released into the environment. Sporangia are attached to hyphae that have been adapted to support their presence. A distinctive physical feature of *P. infestans* is a sporangiophore that branches and has swellings at the border where the sporangia are attached. Sexual spores in fungus are called oospores.

*A. solani* is classified as a Deuteromycete since its sexual stages are either nonexistent or unknown. The fungus produces a greyish-black, cottony, hairy colony when grown in solid media. When septate mycelia are kept for an extended period of time, they take on a dark color. *A. solani*'s sporulation phase may be triggered by exposure to light during culture. Conidiophores

Arvind Singh Negi,

Evaluation of the Mycogenic Biosynthesis of Silver Nanofungicides' Efficacy against Blight Disease Infestations of *Phytophthora Infestans* and *Alternaria Soloni* in Potato *Solanum Tuberosum*

are the structures that produce the asexual spores known as conidia. The conidia have a beaked end and 4-11 transverse septae.

*A. versicolor*'s smooth conidiophores may range in length from 200 to 500 microns; they are produced by the fungus's septate hyphae. On the biserial conidial heads, erupting metulae and phialides are seen. The conidia have a spherical shape. Possible resemblance to *Penicillium* species in the cap form of the conidia.

*Fungus oxysporum* Growing mycelia on solid medium results in a white appearance at first, followed by a purple hue and, in some cases, orange sporodochia. They may also be seen as see-through or very dark blue. The asexual conidiophores begin as singular structures with lateral monophialides and develop into highly branching groups. Canoe-shaped fusiform, slightly curved, pointed-tipped, and aseptate macroconidia best describe this fungus. They range in size from 5 to 13  $\mu$ m, may be terminal or intercalary, and can have a smooth or rough outside wall.

## 4.2 Study of microbe-metal interaction mechanism through UV-Vis spectroscopy and FTIR.

### 4.2.1 Detection of Microbe-Metal Interaction through UV-Vis Spectroscopy

Test and control flasks were subjected to UV-Vis spectral analysis for a full 120 hours. The results of spectral analysis conducted on test and control samples over a period of 96 hours. There was a peak at 210 nm in the *A. flavus* control sample, but none in the *A. niger* sample. Silver nitrate solution with biomass test samples showed peaks outside of the control sample's range between 330 and 360 nm and 380 and 450 nm. The former is a result of the creation of silver nanoparticles, whereas the latter is equivalent to inorganic phosphate. Samples of zinc oxide nanoparticles showed peaks matching to zinc oxide nanoparticles (240 nm to 290 nm) as well as peaks belonging to inorganic phosphates. It was deduced from these findings that inorganic phosphate synthesis could be related to nanoparticle formation. It has been shown in plants that the nitrate reductase enzyme, which is responsible for reducing silver to the nanoparticle form, goes through a phosphorylation/dephosphorylation process when it is dormant and when it is active. Fungi, and particularly the species *Aspergillus*, may use a similar method.



Arvind Singh Negi,

Evaluation of the Mycogenic Biosynthesis of Silver Nanofungicides' Efficacy against Blight Disease Infestations of *Phytophthora Infestans* and *Alternaria Solani* in Potato *Solanum Tuberosum*

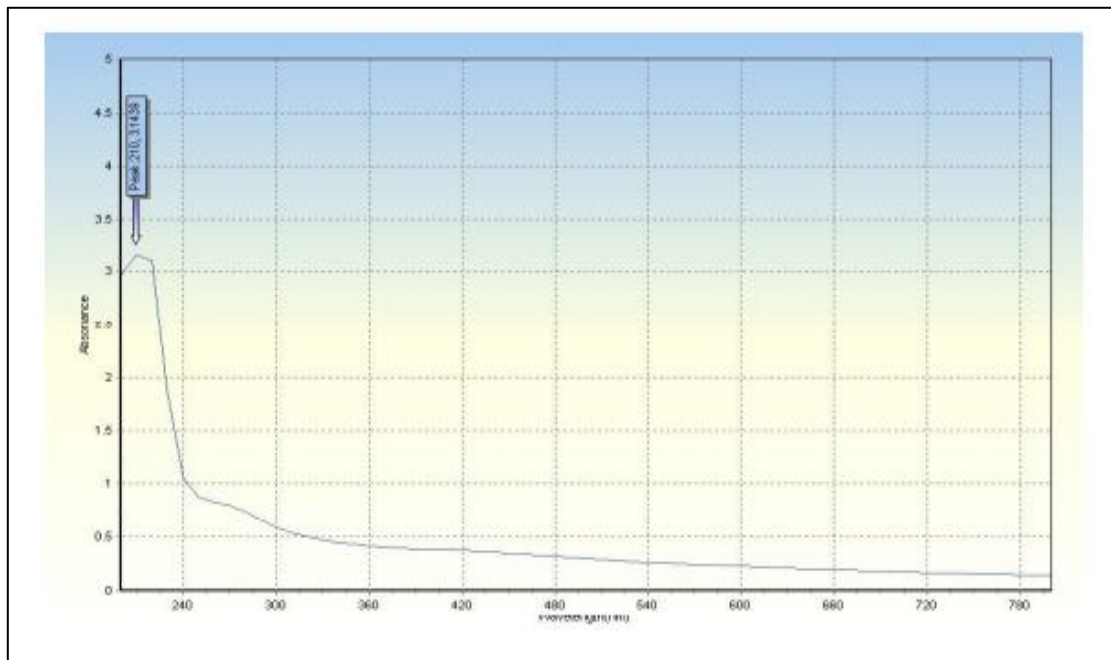


Figure 4.1: Absorbance peaked at 210 nm in the 96-hour spectral report of the AF control

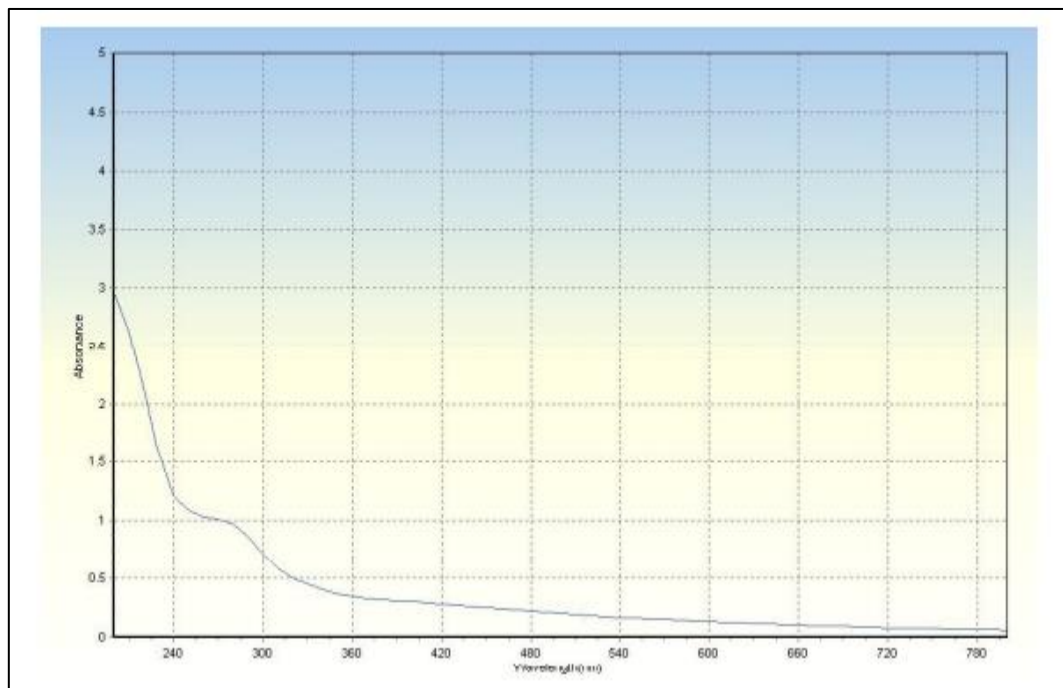


Figure 4.2: AN control spectral report with no peaks after 96 hours

Arvind Singh Negi,

Evaluation of the Mycogenic Biosynthesis of Silver Nanofungicides' Efficacy against Blight Disease Infestations of *Phytophthora Infestans* and *Alternaria Solani* in Potato *Solanum Tuberosum*

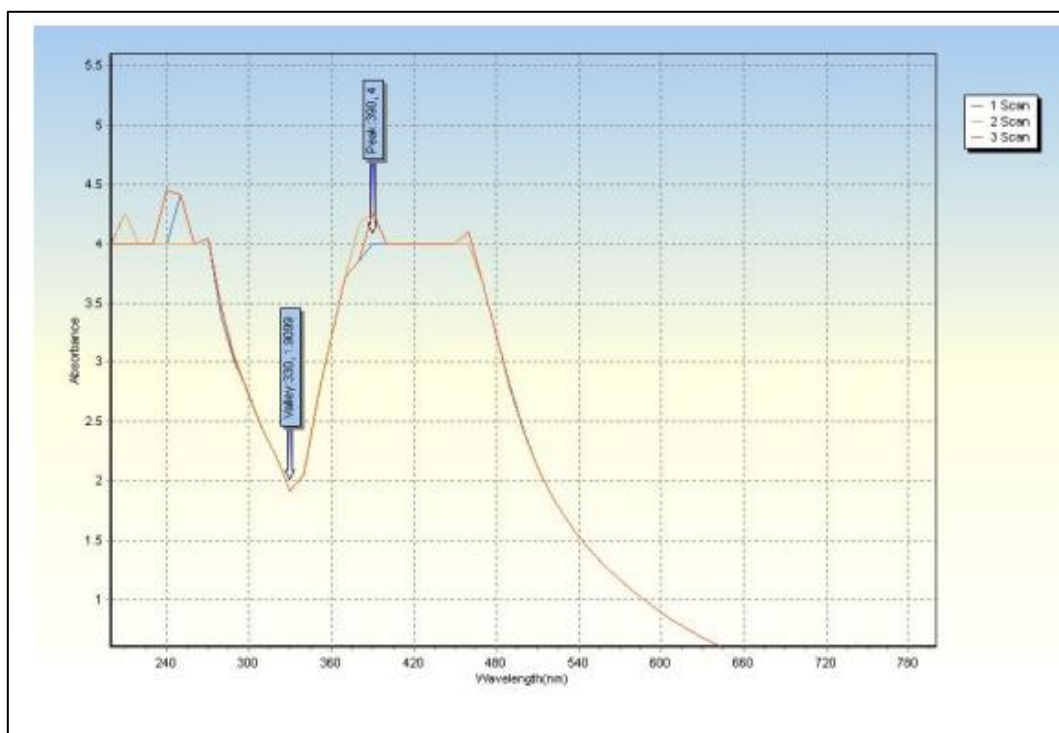


Figure: 4.3: After 96 hours, *Aspergillus flavus* (100 mg) 2mM AgNPs test sample spectrum includes inorganic phosphate and AgNPs peaks at 330 and 390 nm.

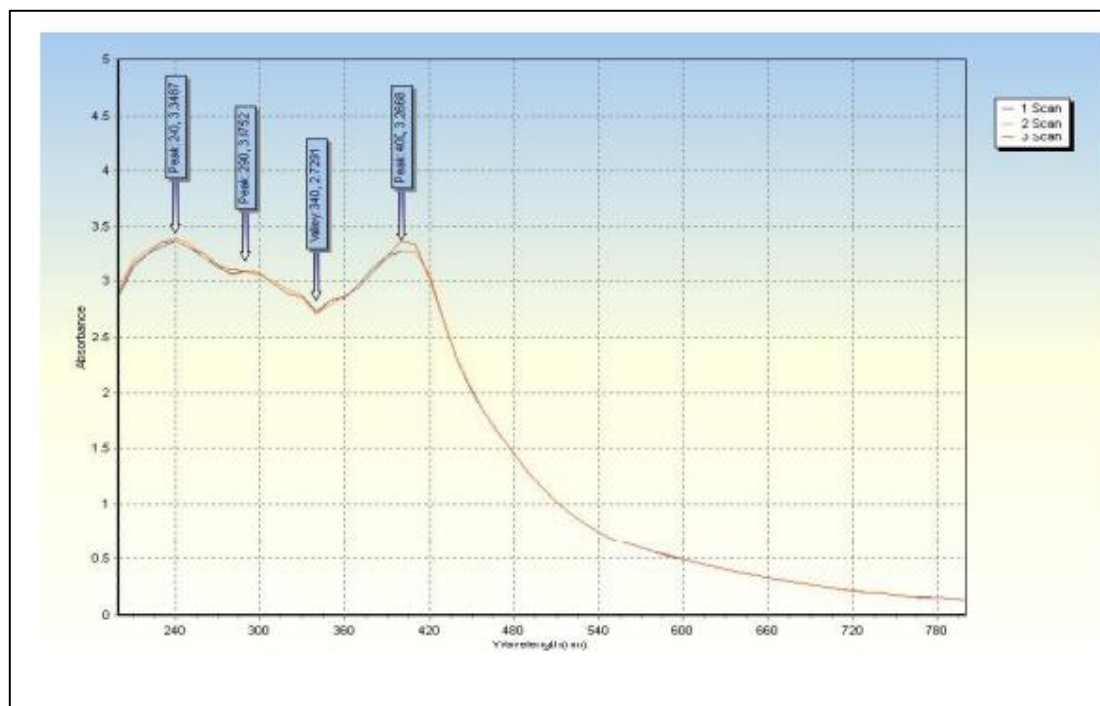


Figure 4.4: *Aspergillus flavus* (1gm) 2mM AgNPs test sample spectrum report after 96 hours, containing inorganic phosphate and AgNPs peaks at 340 and 400 nm.

Arvind Singh Negi,

Evaluation of the Mycogenic Biosynthesis of Silver Nanofungicides' Efficacy against Blight Disease Infestations of *Phytophthora Infestans* and *Alternaria Soloni* in Potato *Solanum Tuberosum*

#### 4.3 Fatty acid region

The profiles of fungal fatty acids in the presence of nanoparticles differed significantly from those of untreated fungus, and the resolution of the peaks in the defined these changes. Observing the peaks at 3100 and 2800 cm allows one to examine the membrane and side-chain vibrations of phospholipids chains through the -CH stretching vibrations of CH<sub>3</sub>, CH<sub>2</sub>, and CH functional groups. Fatty acid peaks were detected in the treated samples of the current investigation, which included AgNPs 2mM (AF-100 mg), AgNPs 2mM (AF-1g), AgNPs 2mM (AF-1g), AgNPs 1mM (AN-1g), and AgNPs 2mM (AN-1g). In the negative control samples, these peaks did not exist. Peaks between 2950 and 2850 cm<sup>-1</sup> are examined for information on CH asymmetric stretching of -CH<sub>3</sub> in fatty acids, CH stretching of >-CH of, CH symmetric stretching of -CH in fatty acids, and CH symmetric stretching of CH<sub>2</sub> in fatty acids. Peak 3015 cm may be used to study the stretching of CH double bonds in unsaturated fatty acid chains, and the spectral bands of fatty acids between 3100 and 2800 cm can be used to assess the severity of membrane nanoparticles.

#### 4.4 Protein region

All treatment samples showed peaks indicative of molecular interactions between fungal proteins and nanoparticles. The amide A and amide B protein N-H stretching maxima were observed to be at 3200 and 3060 cm, respectively. Amide I and II of proteins and peptides dominate the spectrum at 1800 and 1500 cm, whereas the amide III band sits at around 1280 cm<sup>-1</sup>. The stretching vibrations of the C=O groups in the  $\alpha$ -helical and  $\beta$ -pleated sheet structures of proteins cause the amide of proteins to peak about 1695–1675 cm. Amide II bands in proteins manifest in the 1550–1520 cm areas and consist of N–H bending and C–N stretching vibrations of the peptide group. Amide I and amide II bands favored the formation of  $\alpha$  or  $\beta$  structures. FTIR may also be used to identify amino acids, such as tyrosine, which has a characteristic spectral peak at 1515 cm.

#### 4.5 Carbohydrates region

After fungal cells were exposed to nanoparticles, alterations were seen in the 900–1200 cm region of the spectrum, which is dominated by the C–O–C and C–O rings in diverse polysaccharides. Peaks at 1153, 1117, 1102, 1058, 993, and 966 cm correspond to the C-O ring and COH vibrations of carbohydrates, which may be found in the area 1120-1140 cm<sup>-1</sup> of the glycosidic bond. The 1140-1000 cm<sup>-1</sup> band was found to have weaker polysaccharide profiles. These spectrum shifts during peroxidation of lipopolysaccharides may be explained by the lipopolysaccharide's asymmetric outer membrane composition and amphipathic molecules. A drop in peak intensity at 1188 cm, which correlates to carbohydrate alterations, was discovered in another investigation, confirming the presence of ROS-induced damage.

Arvind Singh Negi,

Evaluation of the Mycogenic Biosynthesis of Silver Nanofungicides' Efficacy against Blight Disease Infestations of *Phytophthora infestans* and *Alternaria solani* in Potato *Solanum Tuberosum*

#### 4.6 Fingerprint region

Unique weak bonds, such as those found in nucleic acids and amino acids like phenylalanine, tyrosine, tryptophan, and other nucleotides, are reflected in the fingerprint, which ranges from wave numbers 900 to 600 cm. These peaks appeared in every sample, including the control. Bacterial strains may be differentiated in the fingerprint area. The fingerprint region isn't the only place where you can see bands that correspond to nucleic acids in microorganisms; C=O stretching of esters in nucleic acids and carbonic acids, and C-O-H in-plane bending in the DNA/RNA backbone, all contribute to these peaks, and an increased band near 1738 cm<sup>-1</sup> can be seen in bacteria treated with nanoparticles due to vibration of the C=O carbonyl group. Increased peaks at 1690 and 1734 cm in exposed bacteria suggest an increase in concentration of C=O bonds in aldehydes and ketones, which may be explained by the peroxidation of nucleic acid chains due to oxidative stress caused by the formation of ROS.

#### 5. Conclusion

In conclusion, encouraging results were found when *Phytophthora infestans* and *Alternaria solani* blight diseases in potato *Solanum tuberosum* were tested against silver nanofungicides synthesized by mycogenic biosynthesis. One possible approach to dealing with these catastrophic illnesses is the use of silver nanoparticles generated by mycogenic biosynthesis. This examine the efficacy of mycogenic AgNPs as fungicides against the bacterium that causes early blight on potatoes (*A. solani*) and the fungus that causes late blight on potatoes (*P. infestans*). This research demonstrates that mycogenic AgNPs are efficient disease-control agents against potato blight. Three phytopathogenic (*P. infestans*, *A. solani*, *Fusarium oxysporum*) and one endophytic (*Aspergillus versicolor*) fungi were found and isolated in total. Among the various combinations of fungal biomass and molar concentrations of salt precursor, the AgNPs synthesised by 1g *A. flavus* and *A. niger* biomass with 2 mM silver nitrate solution produced the finest sized nanoparticles and demonstrated the lowest MIC against *P. infestans* and *A. solani*.

#### 6. References

1. Abbas, A., Naz, S.S. and Syed, S.A., (2015). Antimicrobial activity of silver nanoparticles (AgNPs) against *Erwinia carotovora* pv. *carotovora* and *Alternaria solani*. *Int J Biosci*, 6(10), pp.9-14.
2. Hameed, S., (2015). Identification of disease free potato germplasm against potato viruses and PCR amplification of potato virus X. *Int. J. Biol. Biotech*, 9(4), pp.335-339.
3. Qadir, A. and Ahmed, R., (2016). Major potato viruses in potato crop of pakistan: A brief review. *Int. J. Biol. Biotech*, 10(3), pp.435-440.

Arvind Singh Negi,

Evaluation of the Mycogenic Biosynthesis of Silver Nanofungicides' Efficacy against Blight Disease Infestations of *Phytophthora Infestans* and *Alternaria Soloni* in Potato *Solanum Tuberosum*

4. Mahmoud, M.A. and Metwaly, H.A., (2015). Biosynthesis of silver nanoparticles using *Fusarium solani* and its impact on grain borne fungi. *Digest Journal of Nanomaterials and Biostructures*, 10(2), pp.655-662.
5. Daròs, J.A. and Mohamed, M.A., (2016). Assessment of protein silver nanoparticles toxicity against pathogenic *Alternaria solani*. *3 Biotech*, 6(2), p.199
6. Abd-El-Khair, H. and Haggag, W.M., (2007) Application of some Egyptian medicinal plant extracts against potato late and early blights. *Res. J. Agric. Biol. Sci*, 3(3), pp.166-175.
7. Agbenin, O.N. and Marley, P.S., (2016). In vitro assay of some plant extracts against *Fusarium oxysporum* f. sp. *lycopersici* causal agent of tomato wilt. *Journal of plant protection research*, 46(3), pp.215-220.
8. Paquot, M. and Rouxhet, P.G., (2021). XPS analysis of chemical functions at the surface of *Bacillus subtilis*. *Journal of colloid and interface science*, 309(1), pp.49-55.
9. Kumar, R. and Sastry, M., (2020). Extra-/intracellular biosynthesis of gold nanoparticles by an alkalotolerant fungus, *Trichothecium* sp. *Journal of Biomedical Nanotechnology*, 1(1), pp.47-53.
10. Supriyanto, G. and Zaidan, A.H., (2019), January. Synthesis of Silver Nanoparticles and the Development in Analysis Method. In *IOP Conference Series: Earth and Environmental Science*, 217(1), p.012005.
11. Oliveira, G. and Góes-Neto, A., (2018). Effectiveness of ITS and sub-regions as DNA barcode markers for the identification of Basidiomycota (Fungi). *BMC microbiology*, 17(1), p.42.
12. Kim, B.I. and Adair, J.H., (2017). Synthesis and characterization of silver nanoparticles by a reverse micelle process. *Metals and Materials International*, 11(4), pp.291-294.